4. *Escherichia coli* RelBE toxin -antitoxin system

4.1. Results

4.1.1. Circular dichroism spectropolarimetry of *Escherichia coli* RelB, RelE and RelBE complex

The far-UV circular dichroism spectra of 0.41 g/L RelB, 0.56 g/L RelE and 0.61 g/L RelBE complex having 79, 101, and 179 amino acids respectively were measured in PBS buffer, pH 7.4 at 25 °C (Figure 4.1, 4.2 and 4.3).

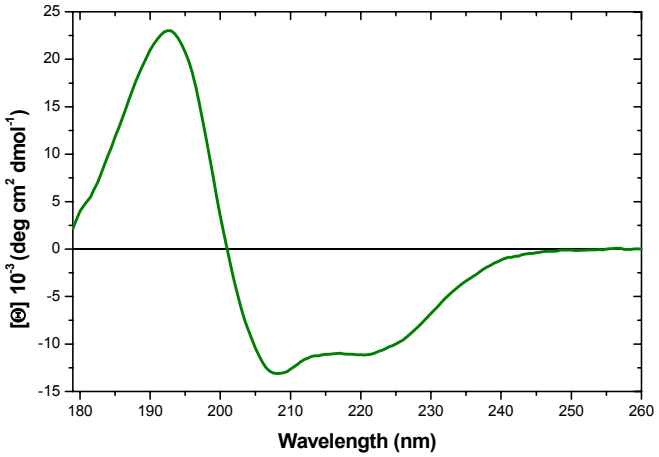

Figure 4.1: Far-UV CD spectra of RelB. Circular dichroism was measured at 25 °C at a concentration of 0.41 g/L RelB in PBS buffer, pH 7.4.

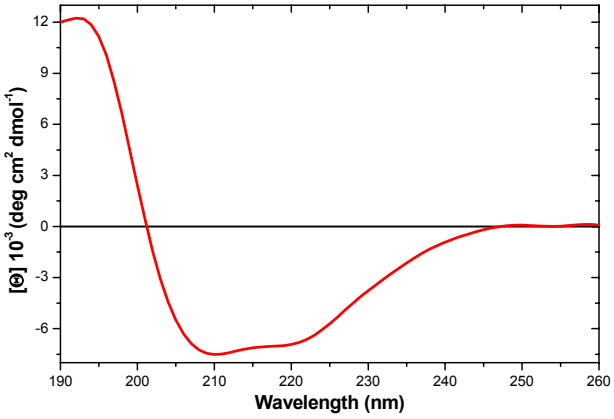

Figure 4.2: Far-UV CD spectra of RelE. Circular dichroism was measured at 25 °C at a concentration of 0.56 g/L RelE, in PBS buffer, pH 7.4.

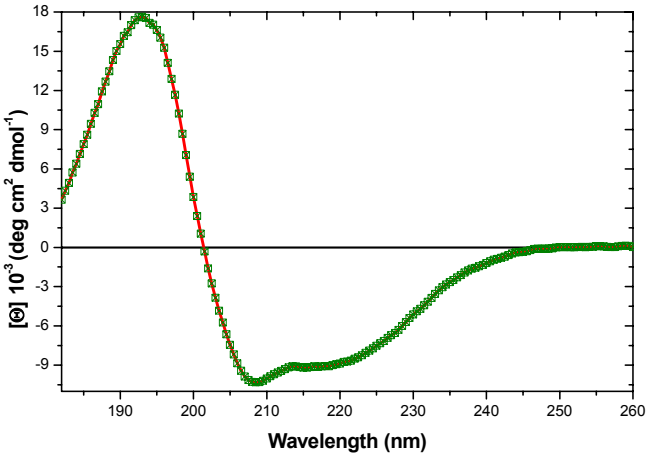

Figure 4.3: Far-UV CD spectra of RelBE complex. Circular dichroism was measured at 25 °C at a concentration of 0.61 g/L RelBE, in PBS buffer, pH 7.4.

Table 4.1: Secondary structure contents of RelB, RelE and RelBE complex.

Protein	α-Helix (%)	β-Sheet (%)	Turn (%)	Remainder (%)	Method
RelB	41 (±0)	28 (±1)	14 (±1)	17 (±2)	CD
RelE	19 (±2)	44 (±2)	17 (±2)	21 (±2)	CD
RelBE Complex	32 (±2)	33 (±2)	17 (±1)	18 (±2)	CD
RelB	50	12	34	4	Prediction
RelE	45	19	33	3	Prediction

As a common characteristic of all spectra (Figure 4.1, 4.2 and 4.3), the strong negative ellipticity revealed minima around ~208 and ~220 nm. Complex RelBE is predominantly composed of a mixture of α-helices (32%) and β-sheets (33%). Antitoxin RelB revealed out to be more of α-helices (41%) as compared to toxin RelE which have only 19% α-helices and 44% β-sheets as calculated with the Variable Selection Method (VARSLC1) (Table 4.1). The calculated VARSLC1 results for RelB are in reasonable agreement with the secondary structure content of 50% α-helices predicted from the amino acid sequence using PHDsec program of the predictProtein package. However, observed RelE secondary

structure differs significantly from prediction. The secondary structure elements are elucidated in Table 4.1.

4.1.2. Hydrodynamic properties and stoichiometry

Hydrodynamic properties and stoichiometry of RelB, RelE and RelBE complex proteins were measured by gel filtration (size exclusion chromatography) and analytical ultracentrifugation experiments. Results obtained for all proteins from experiments are sequentially described as follows:

4.1.2.1. Size exclusion chromatography

4.1.2.1.1. Antitoxin RelB mass determination

Gel filtration experiments were performed at concentration of 0.070 g/L and 1 g/L RelB in PBS buffer, pH 7.4, 25 °C. The elution peak of RelB at both concentrations has an asymmetric shape, with tails to higher elution volumes. The observed apparent molecular masses of RelB are ~11 kDa and ~21.5 kDa for an input concentration of 0.070 g/L and 1 g/L; corresponding to 7.8 μM RelB in monomer equivalents and 55.1 μM $RelB_2$ in dimer equivalents respectively (Figure 4.4). The observed molecular masses exceeded the theoretical molecular mass of a monomer (RelB; 8940.29 Da) and dimers ($RelB_2$; 17880.58 Da). The elution behaviour could indicate that at the lower protein concentration besides a majority of monomers also dimers exist whereas at 1 g/L besides of a majority of dimers also higher oligomeric forms may exist; alternatively, deviations from the globular shape could contribute the high apparent molecular masses.

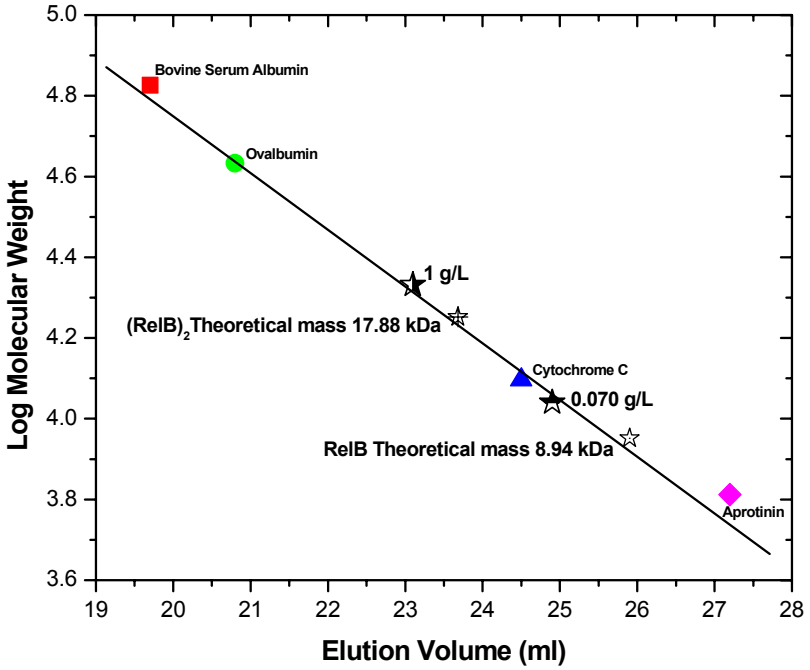

Figure 4.4: Molecular mass determination of RelB by size exclusion chromatography. Molecular standards for calibration were: Bovine serum albumin (67 kDa); Ovalbumin (43 kDa); Cytochrome C (12.5 kDa) and Aprotinin (6.5 kDa).

4.1.2.1.2. Toxin RelE mass determination

Gel filtration experiments were performed at concentration of 0.08 g/L and 0.60 g/L RelE in PBS buffer, pH 7.4, 25 °C. These concentrations correspond to 6.6 μM RelE and 24.90 μM $RelE_2$. The elution peaks of RelE and $RelE_2$ has an asymmetric shape, with tails to higher elution volumes. The peak positions indicated apparent molecular masses of approximately 16,200 Da and 27,500 Da, respectively (Figure 4.5). The observed molecular masses significantly exceeded the theoretical molecular mass of monomers (RelE; 12048.06 Da) and dimers ($RelE_2$; 24096.12 Da). Similar to RelB, the deflected elution behaviour could indicate that at the low concentration besides a majority of monomers dimers also exist, whereas at 0.60 g/L besides dimers also higher oligomeric

forms may exist; alternatively, deviations from the globular shape could contribute to the high apparent molecular masses.

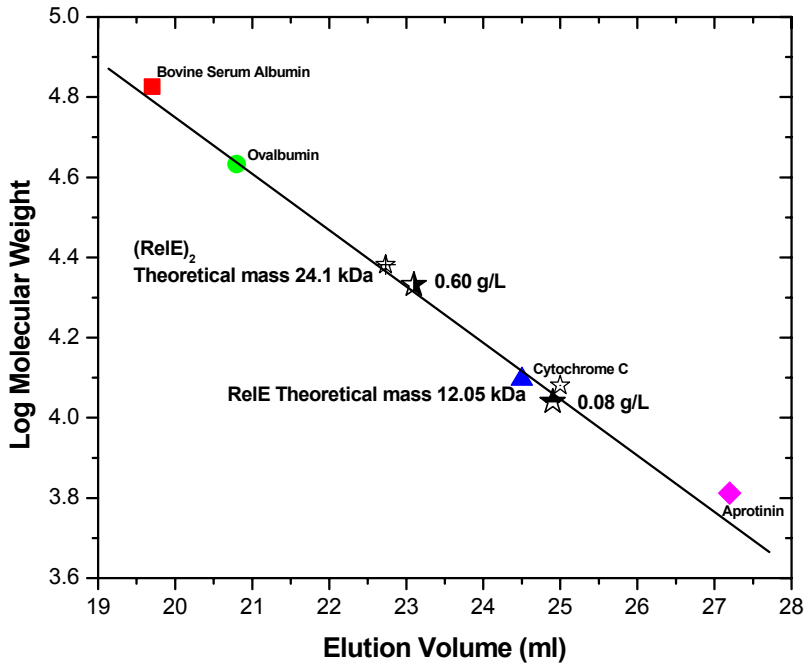

Figure 4.5: Molecular mass determination of RelE by size exclusion chromatography. Molecular standards for calibration were as given in Figure 4.4.

4.1.2.1.3. Toxin -antitoxin RelBE complex mass determination

Gel filtration experiments were performed at concentration of 0.1 g/L and 1.8 g/L RelBE complex in PBS buffer, pH 7.4, 25 °C. These concentrations correspond to 4.8 μM RelBE and 42.9 μM $(RelBE)_2$, respectively. The elution peak of RelBE complex and $(RelBE)_2$ complex has an asymmetric shape, with tails to higher elution volumes. The peak positions indicated apparent molecular masses of approximately 26,500 Da and 43,650 Da, respectively (Figure 4.6). The observed molecular masses exceeded the theoretical molecular mass of a monomeric hetero-complex [RelBE; 20988.4 Da] and are close to that of dimeric hetero-complex [$(RelBE)_2$; 41976.8 Da]. The elution behaviour at the lower

concentration could indicate that besides a majority of monomeric complex also some dimeric complex exists, whereas at the higher concentration almost exclusively dimeric complex exists.

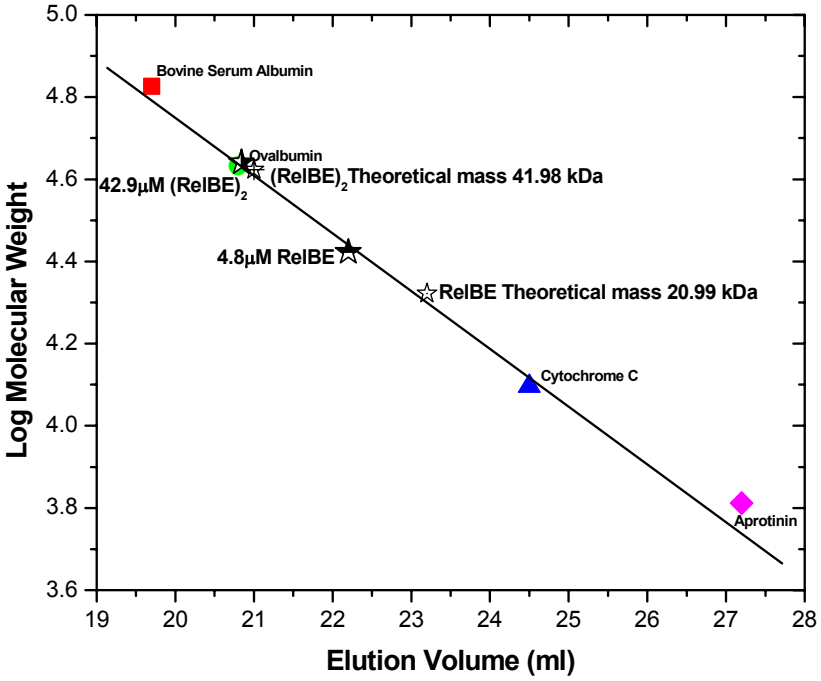

Figure 4.6: Molecular mass determination of RelBE complex by size exclusion chromatography. Molecular standards for calibration were as Figure 4.4.

4.1.2.2. Analytical ultracentrifugation

4.1.2.2.1. Antitoxin RelB mass determination

Analytical ultracentrifugation experiments were performed in the concentration range of 23.15 μM to 55.12 μM $RelB_2$ in PBS buffer, pH 7.4. Experiment revealed molecular masses in the range of 19 kDa – 24 kDa (Figure 4.7). Result addressed the presence of significant amount of dimers up to the concentration of 55.12 μM $(RelB)_2$. Analytical ultracentrifugation data analysis for

concentrations lower than 23.15 μM was not possible due to high signal to noise ratio.

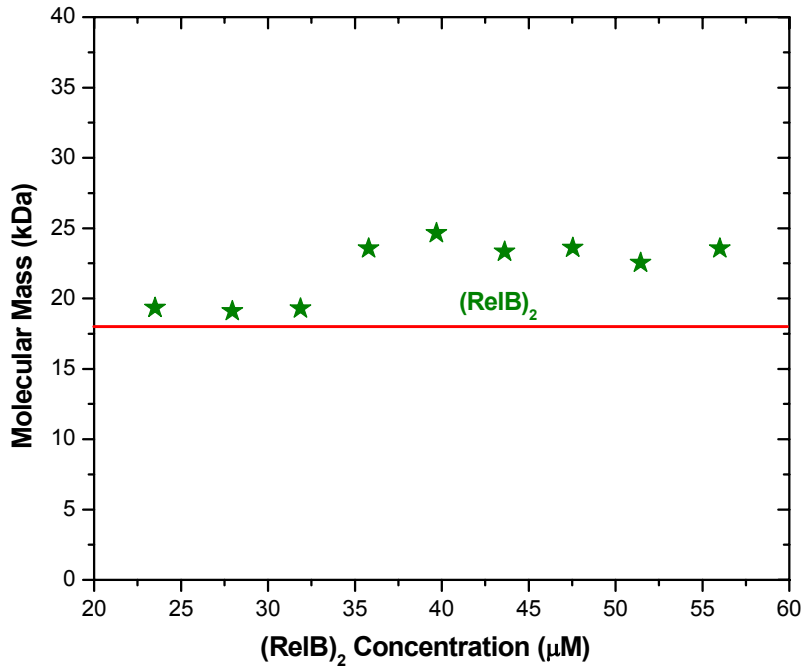

Figure 4.7: Molecular mass determination of RelB by analytical ultracentrifugation. The green stars represent RelB protein in PBS buffer pH 7.4 at respective molar concentrations presented on x-axis. Horizontal red line indicates the theoretical molecular mass of 17.88 kDa for $RelB_2$ (dimer equivalent).

4.1.2.2.2. Toxin RelE mass determination

Analytical ultracentrifugation experiments performed in the concentration range 9 μM to 32.4 μM $RelE_2$ in PBS buffer, pH 7.4, revealed molecular masses in the range of 23 kDa – 24.7 kDa (Figure 4.8). Result addressed the presence of significant amount of dimers in the measured concentration range. Between 4.6 μM and 9 μM increased molecular masses were observed pointing towards aggregation effects at low concentration during experimental run; however high signal to noise ratio complicated the data evaluation.

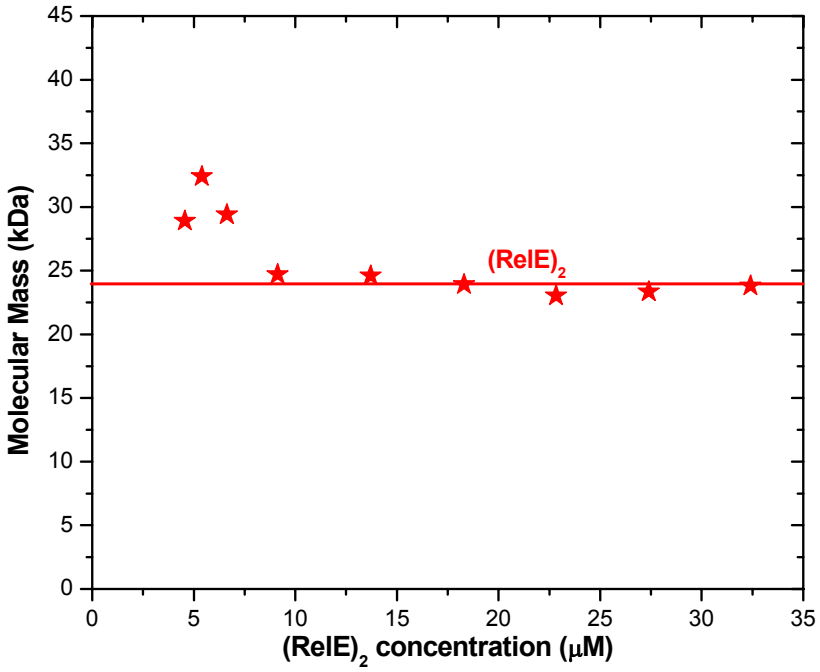

Figure 4.8: Molecular mass determination of RelE by analytical ultracentrifugation. The red stars represent RelE protein in PBS buffer pH 7.4 at its respective molar concentrations presented on x-axis. Horizontal red line indicates the theoretical molecular mass of 24.1 kDa for $RelE_2$ (dimer equivalent).

4.1.2.2.3. Toxin -antitoxin RelBE complex mass determination

Analytical ultracentrifugation experiments were performed in the concentration range 2 μM to 34 μM $(RelBE)_2$ complex in PBS buffer, pH 7.4. Results revealed concentration-dependent molecular masses in the range of 27 kDa – 41 kDa reflecting monomeric-dimeric hetero-complex equilibrium (Figure 4.9).

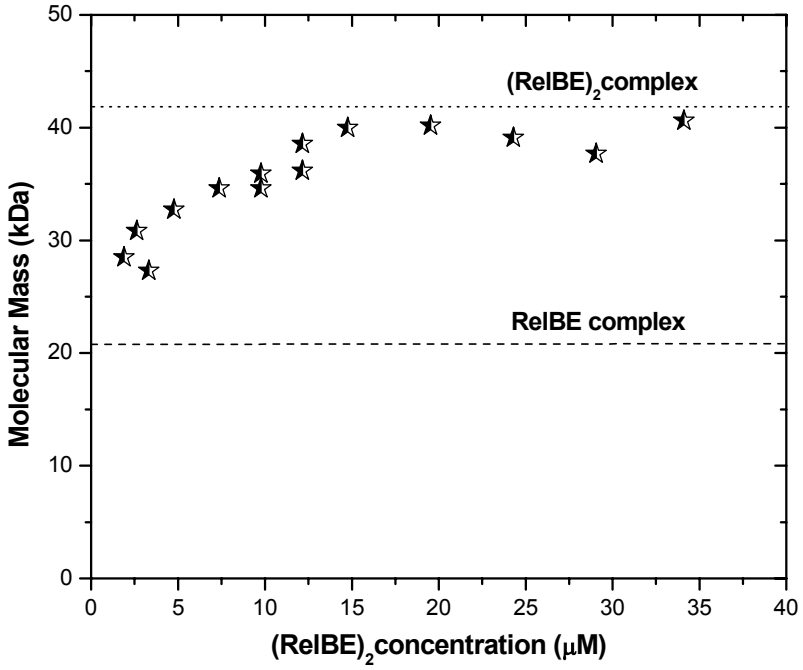

Figure 4.9: Molecular mass determination of RelBE complex by analytical ultracentrifugation. The semi-black stars represent RelBE complex in PBS buffer pH 7.4 at respective molar concentrations presented on x-axis. Horizontal dashed and dotted lines indicate the theoretical molecular mass of 20.99 kDa and 41.98 kDa for RelBE (Hetero-dimer equivalent) and $(RelBE)_2$ (Hetero-tetramer equivalent) respectively.

4.1.3. Denaturant-induced unfolding

Denaturant unfolding of RelB, RelE and RelBE complex was analyzed by monitoring changes in both the far ultraviolet circular dichroism (predominantly secondary structure) and intrinsic fluorescence emission (predominantly tertiary structure). Results from both techniques applied on samples are described below:

4.1.3.1. Circular dichroism

Circular dichroism technique was employed in the analysis of the unfolding of RelB, RelE and RelBE complex, as a spectroscopic probe that is

sensitive to protein secondary structure. As the CD spectra of the RelB, RelE and RelBE complex revealed greater negative ellipticity in the region of 208-230 nm, a region with bands characteristic of α-helix and β-turns. Therefore; unfolding of RelB, RelE and RelBE complex by Gdn-HCl was monitored measuring changes of the CD signal at 220 nm.

4.1.3.1.1. Antitoxin RelB Gdn-HCl induced unfolding

Denaturation curves of RelB at concentration 0.056 g/L and 0.4 g/L RelB points towards a concentration dependent two-state unfolding mechanism (Figure 4.10). Observed transition curves were found to be steeper for low concentration 0.056 g/L as compared to high concentration 0.4 g/L RelB. At low concentration, transition region started at about 1 M Gdn-HCl concentration and continued till the plateau values were reached at 3.3 M Gdn-HCl whereas; at high concentration, pre-transition region was from 0 to 1.5 M Gdn-HCl. Transition region was observed between 1.5 and 5 M Gdn-HCl where the ellipticity decreased from ~ –4.2 millidegrees to ~ –0.7 millidegrees.

Denaturation curves for 0.056 g/L and 0.4 g/L RelB were fitted with two-state monomer and two-state dimer unfolding model [Chapter 9, Appendices; Section 9.1.1. (A) and 9.1.2. (A)] using non-linear least square fitting procedure (Figure 4.11 and 4.12), resulted ΔG, *m* and $C_{½}$ values are presented in Table 4.2.

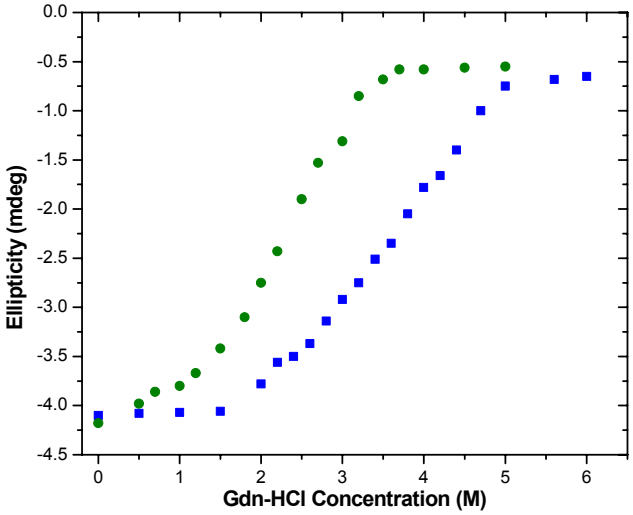

Figure 4.10: Gdn-HCl induced unfolding curve of RelB as monitored by circular dichroism. Gdn-HCl induced unfolding of 0.056 g/L and 0.4 g/L RelB are represented by green circles and blue squares, respectively. PBS buffer, pH 7.4 containing Gdn-HCl concentrations as indicated. CD ellipticity changes were measured at 220 nm and 20 °C.

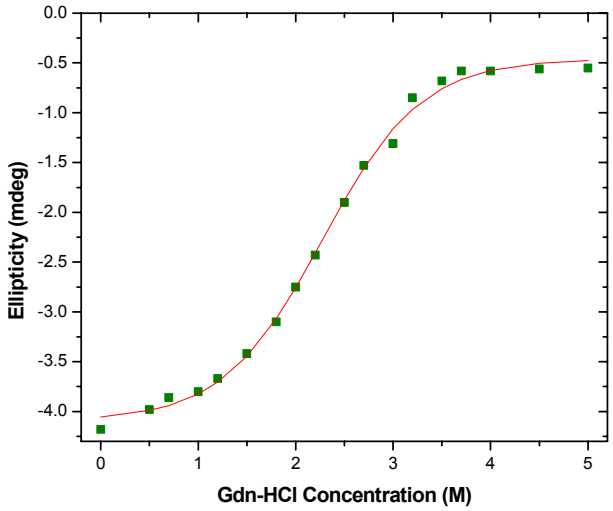

Figure 4.11: Fit for the Gdn-HCl induced unfolding curve of 0.056 g/L RelB as monitored by circular dichroism. Experimental data are represented by green squares. The solid red line represents fit curve according to **two-state monomer unfolding model**. The concentration corresponds to 6.3 μM monomeric RelB (However, presence of dimers can not be excluded). PBS buffer, pH 7.4 containing Gdn-HCl concentrations were used for unfolding as indicated. CD ellipticity changes were measured at 220 nm and 20 °C.

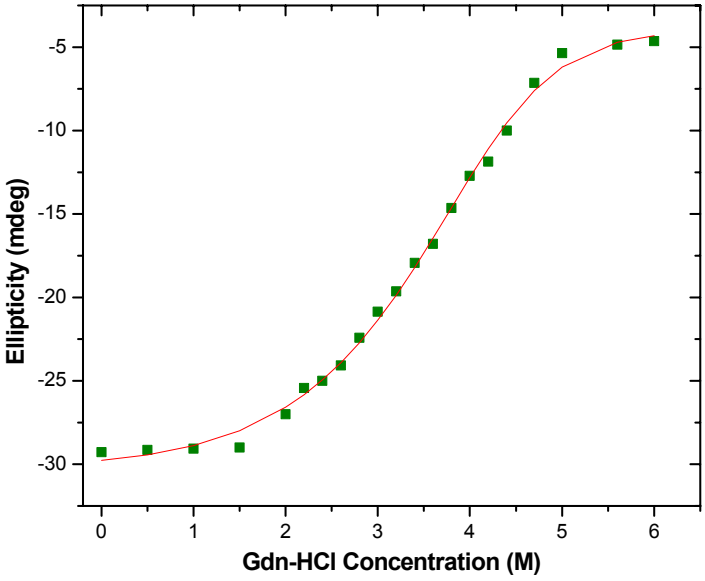

Figure 4.12: Fit for the Gdn-HCl induced unfolding curve of 0.4 g/L RelB as monitored by circular dichroism. Experimental data are represented by green squares. Unfolding curve was factorized to low concentration of 0.056 g/L (Figure 4.11). The solid red line represent fit curve according to **two-state dimer unfolding model**. Protein concentration in dimer equivalents correspond to 22.4 μM $RelB_2$. PBS buffer, pH 7.4 containing Gdn-HCl concentrations as indicated. CD ellipticity changes were measured at 220 nm and 20 °C.

4.1.3.1.2. Toxin RelE Gdn-HCl induced unfolding

Denaturation curves of RelE at concentration 0.082 g/L and 0.4 g/L RelE points towards a concentration dependent two-state unfolding mechanism. Observed transition curves were found to be steeper for high concentration (0.4 g/L) as compared to low concentration (0.082 g/L). At low concentration transition region starts from ~-5 millidegrees corresponding to ~1 M Gdn-HCl and continues till the plateau values are reached at -0.8 millidegrees and 4.4 M Gdn-HCl (Figure 4.14), whereas; at high concentration, from 0 to 3.3 M Gdn-HCl the ellipticity changes hardly exceeded the experimental error of the data. A steep transition region was observed between 3.4 and 4.5 M Gdn-HCl where the ellipticity decreased from ~ –8.2 millidegrees till the plateau value of ~ –1.5 millidegrees

(Figure 4.15). In Figure 4.13, transition curves are factorized to 1 g/L to provide virtuous comparison of high and low concentration.

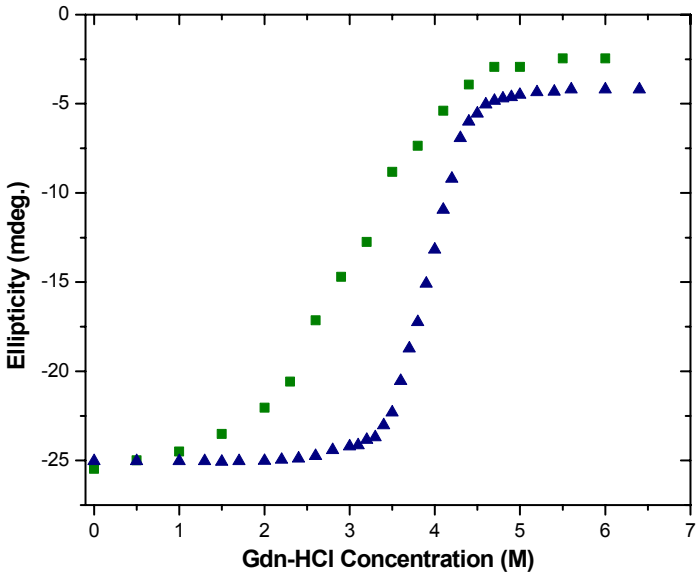

Figure 4.13: Gdn-HCl induced unfolding of RelE for comparison as monitored by circular dichroism. Gdn-HCl induced unfolding of 0.082 g/L and 0.4 g/L RelE are represented by green squares and blue triangles, respectively. For comparison, experimental curves were factorized to 1 g/L concentration. PBS buffer, pH 7.4 containing Gdn-HCl concentrations were used for unfolding as indicated. CD ellipticity changes were measured at 220 nm and 20 °C.

Denaturation curve for 0.082 g/L corresponding to 6.8 μM RelE monomer equivalent and 0.4 g/L to 16.6 μM $RelE_2$ dimer equivalent were fitted with two-state monomer and two-state dimer unfolding model [Chapter 9, Appendices; Section 9.1.1. (A) and 9.1.2. (A)] using non-linear least square fitting procedure (Figure 4.14 and 4.15) resulted ΔG, *m* and $C_{½}$ values as presented in Table 4.2.

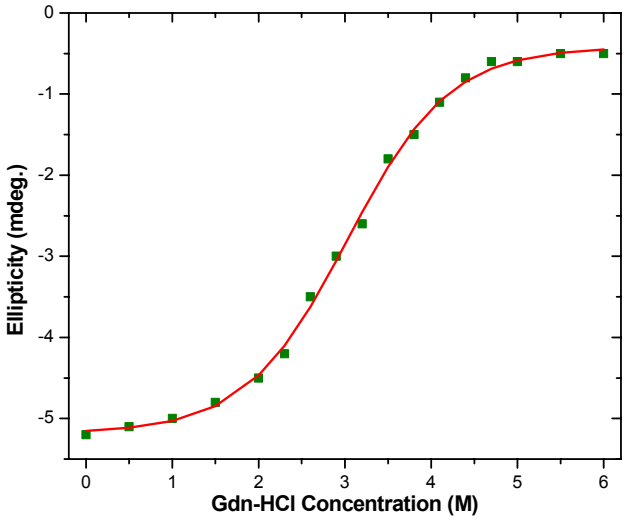

Figure 4.14: Fit for the Gdn-HCl induced unfolding curve of 0.082 g/L RelE as monitored by circular dichroism. Experimental data is represented by green squares. The solid red line represents fit curve according to **two-state monomer unfolding model**. Protein concentration corresponds to 6.8 μM RelE monomer. PBS buffer, pH 7.4 containing Gdn-HCl concentrations were used for unfolding as indicated. CD ellipticity changes were measured at 220 nm and 20 °C.

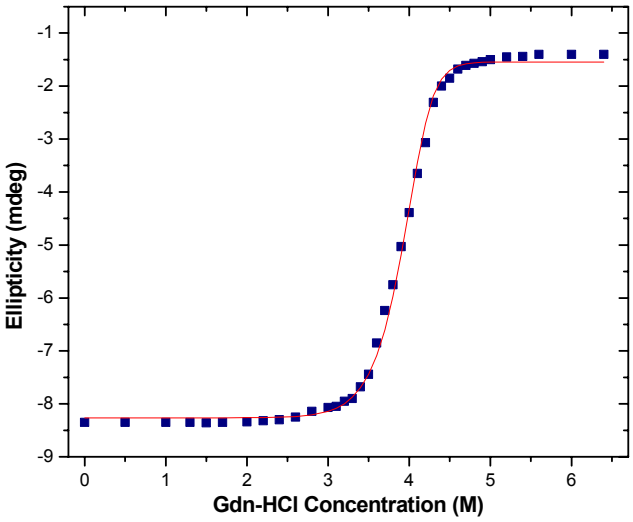

Figure 4.15: Fit for the Gdn-HCl induced unfolding curve of 0.4 g/L RelE as monitored by circular dichroism. Gdn-HCl induced unfolding of 16.6 μM (0.4 g/L) $RelE_2$ is represented by blue squares. The solid red line represent fit curve according to **two-state dimer unfolding model**. Protein concentration in dimer equivalents corresponds to 16.6 μM $RelE_2$. PBS buffer, pH 7.4 containing Gdn-

HCl concentrations were used for unfolding as indicated. CD ellipticity changes were measured at 220 nm and 20 °C.

4.1.3.1.3. Toxin -antitoxin RelBE complex Gdn-HCl induced unfolding

Denaturation curves of RelBE complex at concentration 0.016 g/L, 0.1 g/L, 0.4 g/L and 0.8 g/L RelBE directs to concentration dependent two-state unfolding (Figure 4.16).

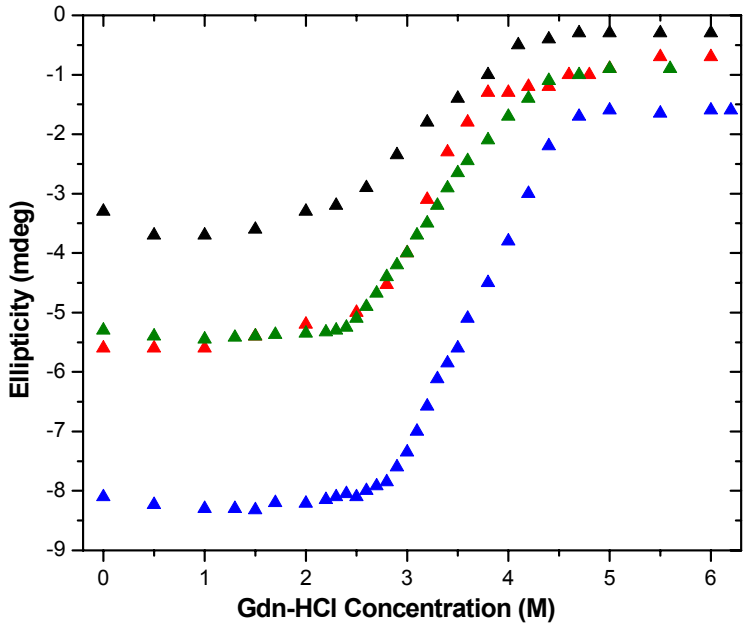

Figure 4.16: Gdn-HCl induced unfolding curves of RelBE as monitored by circular dichroism. Gdn-HCl induced unfolding of 0.016 g/L, d= 0.5 cm; 0.1 g/L, d= 0.1 cm; 0.4 g/L, d= 0.02 cm; and 0.8 g/L, d= 0.02 cm; are represented by black, red, green and blue triangles, respectively. PBS buffer, pH 7.4 containing Gdn-HCl concentrations as indicated. CD ellipticity changes were measured at 220 nm and 20 °C.

In Figure 4.17, assuming two-state unfolding, denaturant curves were normalized to fraction unfolded. For 0.016 g/L, 0.1 g/L, 0.4 g/L, and 0.8 g/L RelBE; ~3.1 M, ~3.2 M, ~3.3 M and ~3.8 M $C_{½}$ values has been calculated respectively. Increase in protein concentration revealed a marginal denaturant stability differences pointing to higher denaturant stability with increase in protein

concentration. Therefore concentration dependence is evident but unfortunately absence of obvious dissociation steps or intermediates in multi-component system could not be seen. Hence calculation of thermodynamic parameters by fitting models was not possible in this case. Only approximate $C_{½}$ values can be determined.

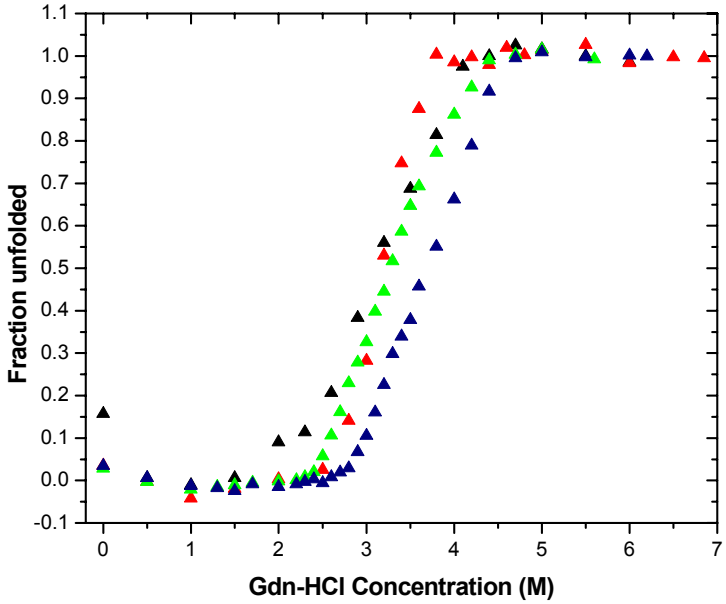

Figure 4.17: Normalized Gdn-HCl induced unfolding curves of RelBE as monitored by circular dichroism. Gdn-HCl induced unfolding of 0.016 g/L, 0.1 g/L, 0.4 g/L and 0.8 g/L RelBE are represented by black, red, green and blue triangles, respectively. For comparison, experimental curves shown in Figure 4.16 were normalized to fraction folded. Buffer 20 mM Tris, 150 mM NaCl, pH 8 containing Gdn-HCl concentrations as indicated. CD ellipticity changes were measured at 220 nm and 20 °C.

4.1.3.2. Fluorescence spectroscopy

4.1.3.2.1. Antitoxin RelB Gdn-HCl induced unfolding

Examination of RelB unfolding by intrinsic tyrosine fluorescence

The fluorescence emission spectrum of RelB in PBS buffer, pH 7.4 has emission maximum near 305 nm as expected for selectively excited tyrosine residues (Figure 4.18).

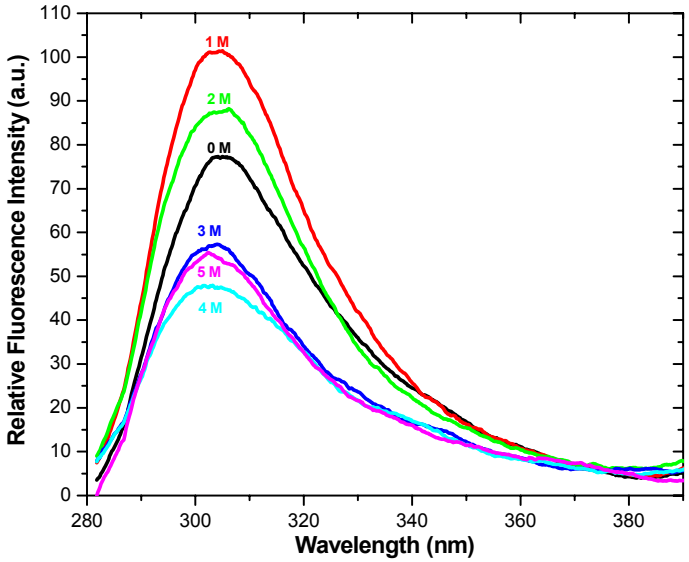

Figure 4.18: Fluorescence emission spectra of RelB at varying Gdn-HCl concentration as indicated in the Figure. Protein concentration was 0.056 g/L RelB in PBS buffer, pH 7.4; Excitation wavelength was 277 nm, measurements at 20 °C.

In RelB monomer, two tyrosine residues and no tryptophan are present. Increasing Gdn-HCl concentrations from 0 to 5 M resulted in increase in fluorescence intensity at 1 M Gdn-HCl followed by a gradual decrease up to 4 M Gdn-HCl suggesting increasing number of exposed tyrosine residues. Result is comparable with the denaturant unfolding measured by CD in Figure 4.11. At 5 M Gdn-HCl, the fluorescence intensity is similar to that at 3 M Gdn-HCl, possibly because of aggregation effects or experimental errors as fluorescence is highly sensitive to protein concentration and proper mixing of samples necessary to avoid precipitates. Moreover, fluorescence spectra showed that the samples were not contaminated by tryptophan containing impurities.

4.1.3.2.2. Toxin RelE Gdn-HCl induced unfolding

RelE monomer contains five tyrosines and most importantly one tryptophan, therefore fluorescence emission spectra of folded RelE in PBS

buffer, pH 7.4 had the maximum near ~324-328 nm as expected for selectively excited tryptophan residues. Tryptophan residue spectra dominated over tyrosine eventhough excitation wavelength was 277 nm specific for tyrosine residue. Excitation in the presence of 6 M Gdn-HCl resulted in splitting of peak into two peaks, characteristic to exposed tyrosines and tryptophan in the hydrophilic environment (Figure 4.19). Similarly RelE in presence of native buffer and different Gdn-HCl concentrations were excited at 295 nm, specifically for tryptophan resulted in gradual decrease of fluorescence intensity with a red shift in peak maxima wavelength (Figure 4.20).

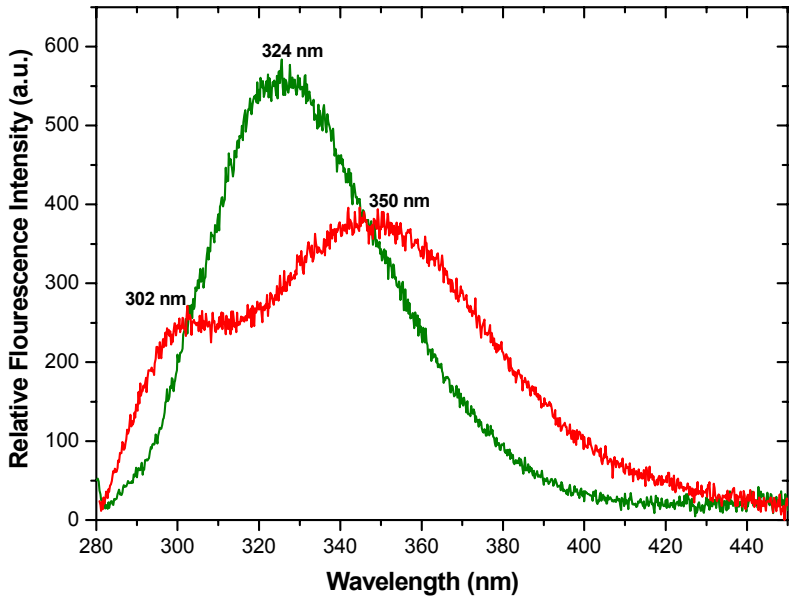

Figure 4.19: Fluorescence emission spectra of RelE in the presence of Gdn-HCl denaturant. Protein concentration was 0.082 g/L RelE in PBS buffer, pH 7.4; Excitation wavelength was 277 nm, measurements at 20 °C. Green and red spectra correspond to the RelE in PBS buffer, pH 7.4 containing 0 M and 6 M Gdn-HCl concentration respectively. The two peaks in 6 M Gdn-HCl at 302 and 350 nm are caused by the fluorescence of tyrosine and tryptophan, respectively.

Denaturation curves of RelE at concentration 0.082 g/L RelE (Figure 4.19, 4.20 and 4.21) and 0.4 g/L RelE (Figure 4.21, spectra not shown) revealed a concentration dependent unfolding. Spectra were measured in the range of 0-6 M

Gdn-HCl concentration. In the absence of Gdn-HCl, emission maximum at ~325 nm was observed as expected from selective tryptophan molecule in hydrophobic environment. At 6 M Gdn-HCl, emission maximum was shifted to 350 nm characteristic for tryptophan molecules exposed to the environment.

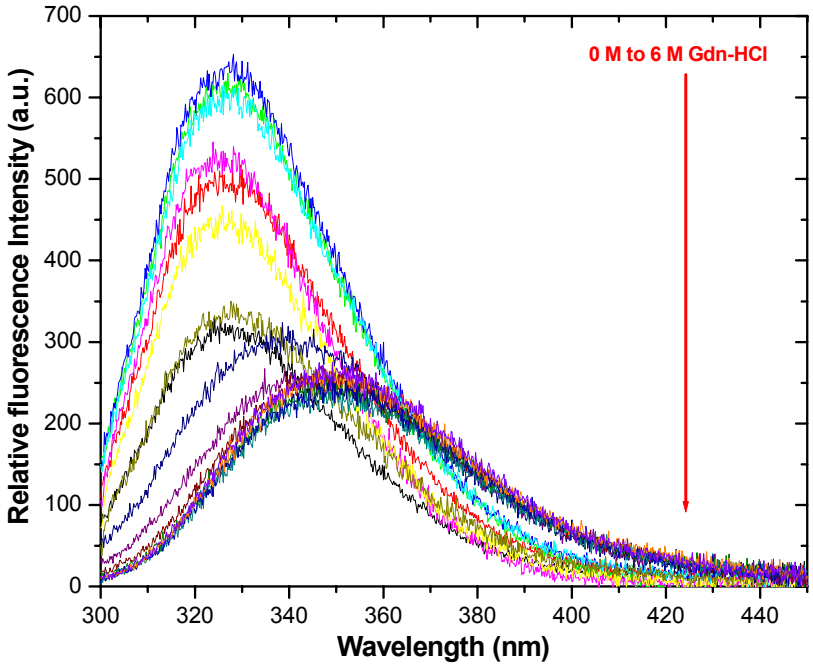

Figure 4.20: Fluorescence emission spectra of RelE at varying Gdn-HCl concentration. Protein concentration was 0.082 g/L RelE in PBS buffer, pH 7.4; Excitation wavelength was 295 nm, measurements at 20 °C.

The emission maxima wavelengths were plotted against respective Gdn-HCl concentration for two protein concentrations (Figure 4.21). Observed transition curves were found to be steeper for high concentration 0.4 g/L as compared to low concentration 0.082 g/L RelE. At low concentration transition region starts with slow increase from 2 M Gdn-HCl followed by a steeper but still moderate increase till the plateau value reached at 4.5 M Gdn-HCl, whereas; at high concentration, from 0 to 3.0 M Gdn-HCl a pretransition region with small increase of the intensity maxima was observed followed by a steep transition region between 3.5 and 4.5 M Gdn-HCl till the plateau values are reached at 4.7

M. In Figure 4.21, transition curves are shifted by a factor to compare with peak maxima wavelength obtained by lower concentration. This provides virtuous comparison of the two unfolding curves obtained at high and low concentration.

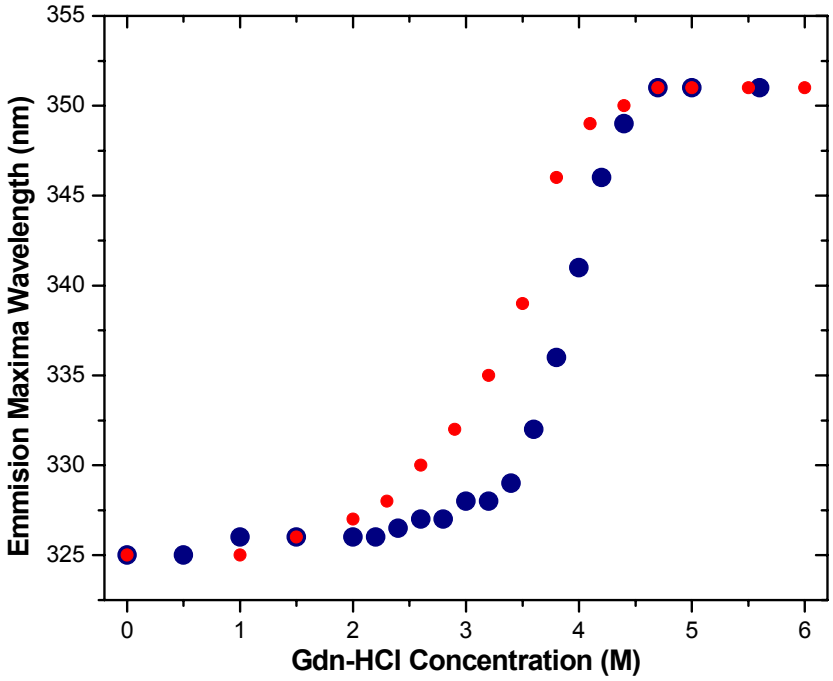

Figure 4.21: Gdn-HCl denaturation curve of RelE as monitored by fluorescence. Experimental data measured at protein concentration of 0.082 g/L and 0.4 g/L RelE are represented by red and blue circles respectively. Change of emission wavelength was plotted on the basis of the shift of emission wavelength maximum at different concentration of Gdn-HCl in PBS, pH 7.4. Curves were shifted to same start as 325 nm.

Denaturation curves obtained for 0.082 g/L corresponding to monomer concentration of 6.8 μM RelE and 0.4 g/L to dimer equivalent of 16.6 μM $RelE_2$ were fitted by two-state monomer and two-state dimer unfolding model [Chapter 9, Appendices; Section 9.1.1. (A) and 9.1.2. (A)]; using non-linear square analysis method (Figure 4.22 and 4.23). Calculated thermodynamic patrameters are summarized in Table 4.2.

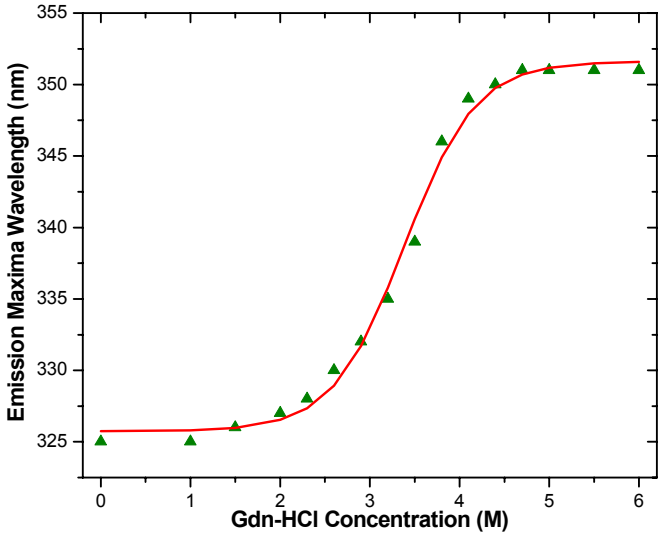

Figure 4.22: Fit for Gdn-HCl induced unfolding curve of 0.082 g/L RelE as monitored by fluorescence. Experimental data are represented by green triangles. The solid red line represent fit curve according to **two-state monomer unfolding model** calculated for a 6.8 μM monomer concentration. PBS buffer, pH 7.4 containing Gdn-HCl concentrations were used for unfolding as indicated. Change of emission maxima wavelengths were measured at 20 °C.

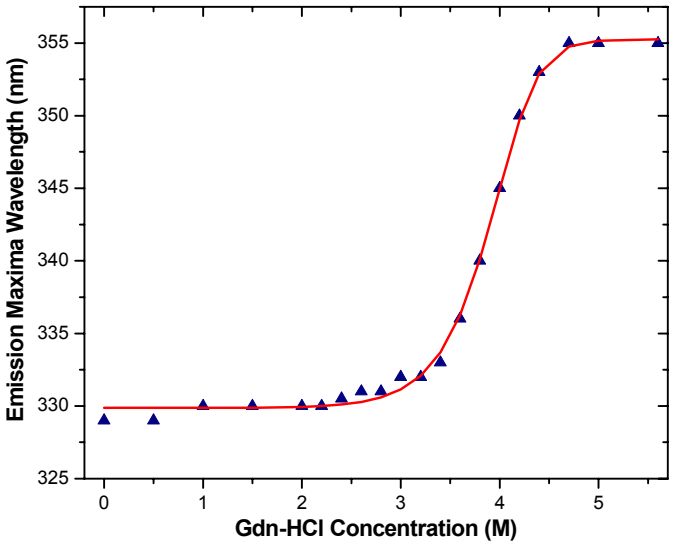

Figure 4.23: Fit for Gdn-HCl induced unfolding curve of 0.4 g/L RelE as monitored by fluoreoscence. Experimental data are represented by blue triangles. The solid red line represent fit curve according to **two-state dimer unfolding model**, calculated for a 16.6 μM dimer equivalent. PBS buffer, pH 7.4

containing Gdn-HCl concentrations as indicated. Change of emission maxima wavelengths were measured at 20 °C.

Table 4.2: Calculated thermodynamic parameters for RelB and RelE by circular dichroism and fluorescence.

Protein	Method	Protein conc. (M) in monomer equivalents used for model fitting	Protein conc. in moles (μM) and grams (g/L)	Denaturant conc. at half unfolding (C½)	ΔG (kcal/ mol)	*m* (kcal /L)	Model
RelB	CD	6.26 E-6 M	6.3 μM RelB or 0.056 g/L	2.3 M	2.6± 0.16	1.14± 0.07	Two-state monomer
RelB	CD	4.47 E-5 M	22.4 μM $RelB_2$ or 0.4 g/L	3.5 M	10.04± 0.24	1.17± 0.06	Two-state dimer
RelE	CD	6.77 E-6 M	6.8 μM RelE or 0.082 g/L	3 M	2.98± 0.14	0.98± 0.04	Two-state monomer
RelE	Fluo	6.83 E-6 M	6.8 μM RelE or 0.082 g/L	3.2 M	4.94± 0.52	1.46± 0.15	Two-state monomer
RelE	CD	3.32 E-5 M	16.6 μM $RelE_2$ or 0.4 g/L	4 M	23.8± 1.6	4.53± 0.4	Two-state dimer
RelE	Fluo	3.32 E-5 M	16.6 μM $RelE_2$ or 0.4 g/L	4 M	19.22± 1.26	3.4± 0.32	Two-state dimer

4.1.3.2.3. Toxin -antitoxin RelBE complex Gdn-HCl induced unfolding

RelBE complex contains seven tyrosines, two from RelB and five for RelE, and most importantly one tryptophan from RelE component of the complex. Excitation at 277 nm reveals emission maxima of tryptophan at 324 nm in buffer containing 0 M Gdn-HCl. In the presence of 6 M Gdn-HCl denaturant in buffer, two emission maxima peaks at 302 and 347 nm corresponding to tyrosine and tryptophan were observed (Figure 4.24).

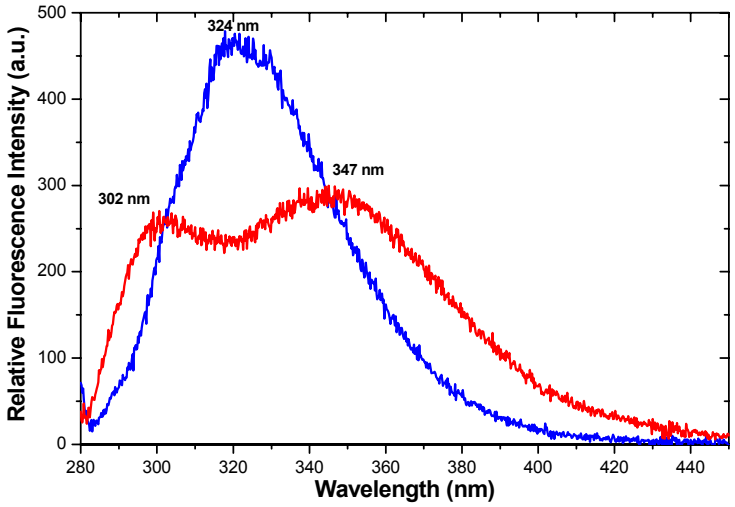

Figure 4.24: Fluorescence emission spectra of RelBE complex in buffer and Gdn-HCl containing buffer. Protein concentration was 0.08 g/L. Excitation wavelength was 277 nm, measurements at 20 °C. Blue and red spectra correspond to RelBE in buffer 20 mM Tris, 150 mM NaCl, pH 8 containing 0 M and 6 M Gdn-HCl concentrations respectively.

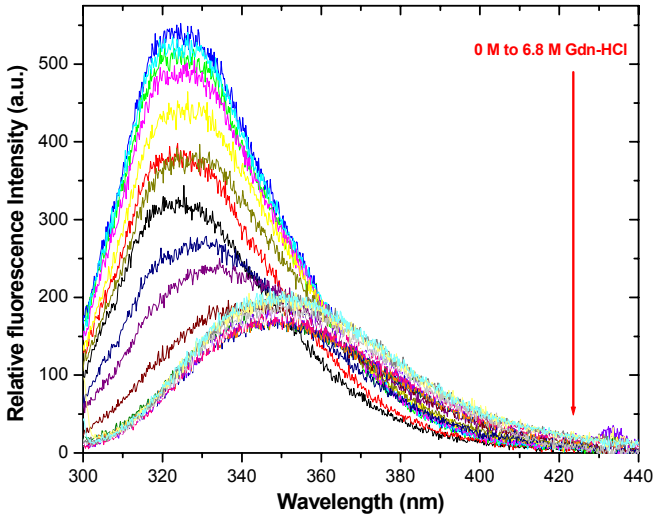

Figure 4.25: Fluorescence emission spectra of RelBE at varying Gdn-HCl concentration in buffer. Protein concentration was 0.08 g/L RelBE in buffer 20 mM Tris, 150 mM NaCl, pH 8 containing 0 M to 6.8 M Gdn-HCl concentrations respectively; Excitation wavelength was 295 nm, measurements at 20 °C.

Denaturation curves of RelBE complex at excitation wavelength of 295 nm in buffer 20 mM Tris, 150 mM NaCl, pH 8 at concentration 0.08 g/L, 0.4 g/L and 0.8 g/L are shown in Figure 4.25 and 4.26.

Emission maxima at different Gdn-HCl concentration were plotted against wavelength, and transition curves were normalized to provide virtuous comparison of measured concentration effects on the shape of the unfolding curves. Observed transition curves were found to be different for low concentration (0.08 g/L) on one side and high concentrations (0.4 and 0.8 g/L) on the other side (Figure 4.26). For 0.08 g/L RelBE, transition region starts from 2.8 M Gdn-HCl and continues to 4.6 M Gdn-HCl whereas, curves measured at 0.4 g/L and 0.8 g/L follow nearly same behaviour. Transition region for both concentration 0.4 g/L and 0.8 g/L starts at 3 M Gdn-HCl and sigmoidal changes continue till the plateau values are reached at 4.8 M Gdn-HCl.

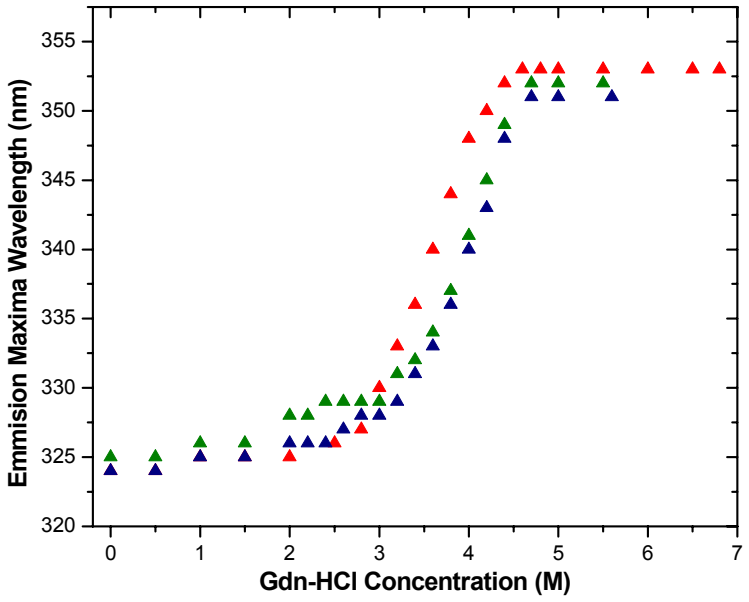

Figure 4.26: Gdn-HCl denaturation curve of RelBE as monitored by fluorescence. Measured concentration 0.08 g/L, 0.4 g/L and 0.8 g/L are represented by red, blue and green triangles, respectively. Change of peak emission wavelength is plotted against concentration of Gdn-HCl in buffer 20 mM Tris, 150 mM NaCl, pH 8.

4.1.3.3. Comparitive analysis of Gdn-HCl unfolding curves obtained from CD and fluorescence measurements.

To check the coincidence in the results obtained by denaturant induced unfolding followed by circular dichroism measuring changes in secondary structure and fluorescence spectroscopy measuring the changes in the environment or surroundings of tryptophan or possibly changes in tertiary structure were compared in Figures 4.27 to 4.31.

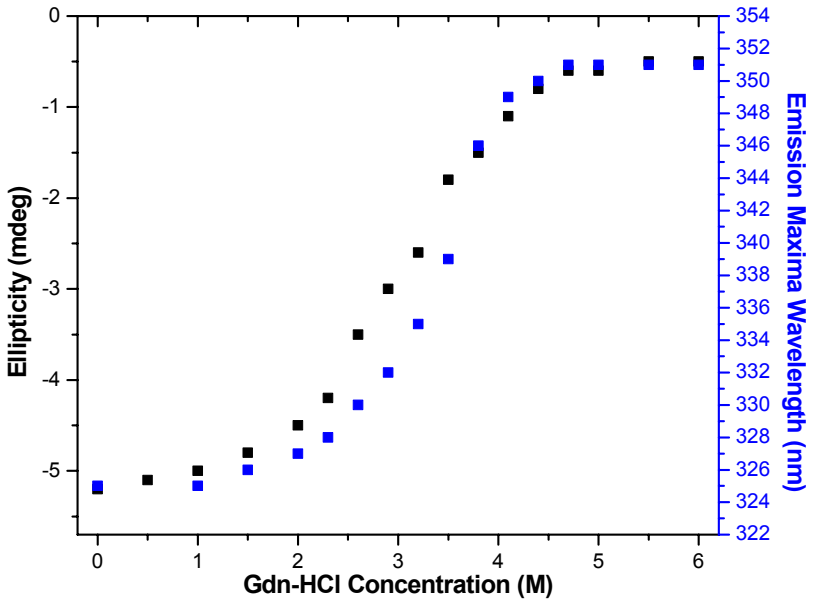

Figure 4.27: Plot of equilibrium unfolding data monitored by circular dichroism and fluorescence for 0.082 g/L RelE. Black and blue squares represent measured ellipticity by CD at 220 nm and emission maxima wavelength by fluorescence with respect to change in Gdn-HCl concentration while excitation was at 295 nm in PBS buffer, pH 7.4.

4.1.3.3.1. Toxin RelE Gdn-HCl induced unfolding

Denaturation curves of RelE at concentration 0.082 g/L and 0.4 g/L RelE obtained from circular dichroism and fluorescence spectrocopy were compared in Figure 4.27 and 4.28, respectively.

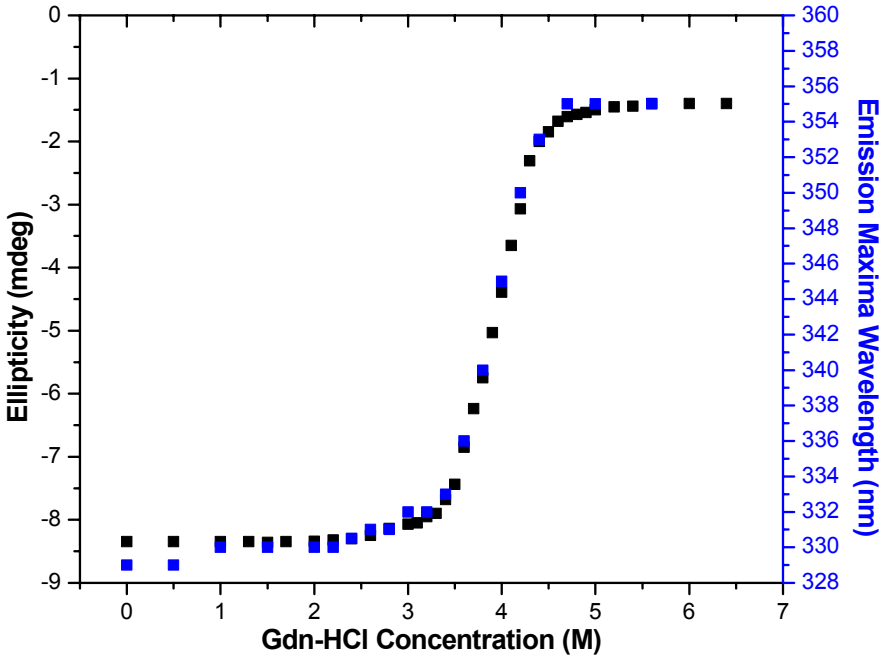

Figure 4.28: Plot of equilibrium unfolding data monitored by circular dichroism and fluorescence for 0.4 g/L RelE. Black and blue squares represent CD and fluorescence data. Fluorescence excitation was at 295 nm in PBS buffer, pH 7.4.

At low concentration (Figure 4.27), unfolding curves measured by CD and fluoroscence differ significantly with a shift to higher denaturant stability observed by fluorescence measurements. At high concentration (Figure 4.28), results obtained from circular dichroism and fluorescence spectroscopy are superimposable.

4.1.3.3.2. Toxin -antitoxin RelBE complex Gdn-HCl induced unfolding

Fluorescence and circular dichroism of RelBE complex can be compared but for interpretation of results we have to keep in mind that RelE is a tryptophan containing component of RelBE complex. By our experiments we are aware that tryptophan is buried inside the RelE molecule, so changes seen in RelBE complex fluorescence are the changes of RelE tryptophan in RelBE complex.

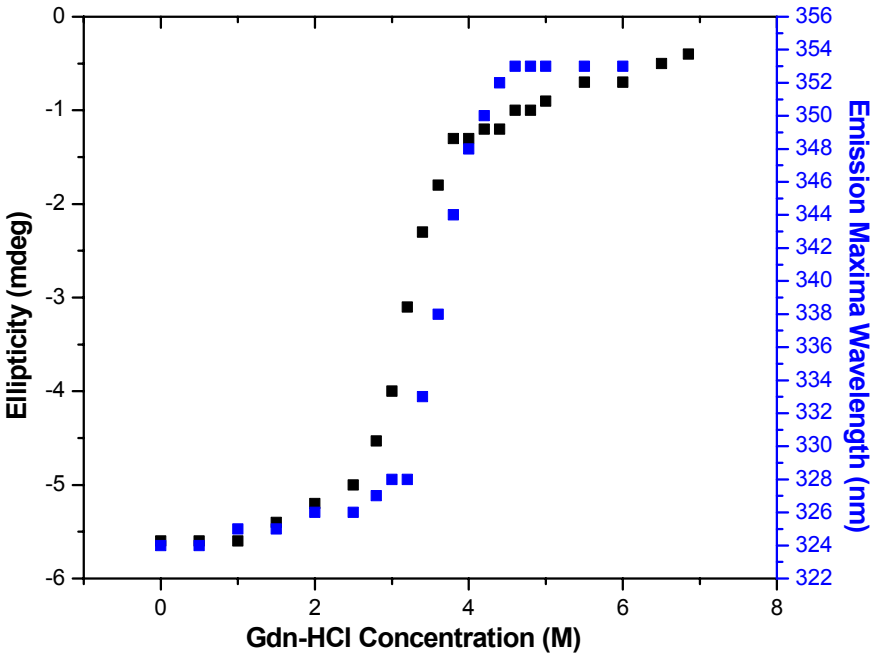

Figure 4.29: Plot of equilibrium unfolding data monitored by circular dichroism and fluorescence for ~0.08 g/L RelBE complex. Black and blue squares represent CD and fluorescence data. Fluorescence excitation was at 295 nm in buffer 20 mM Tris, 150 mM NaCl, pH 8.

In Figure 4.29, 4.30 and 4.31, results for ~0.08 g/L, 0.4 g/L and 0.8 g/L RelBE, used in fluorescence and circular dichroism, respectively are compared. CD monitored unfolding shows a slightly lower denaturant stability as compared to the RelBE fluorescence curves (Figure 4.29, 4.30 and 4.31). A small shift in fluorescence transition curve towards higher denaturant stability points to higher stability of RelE in RelBE complex.

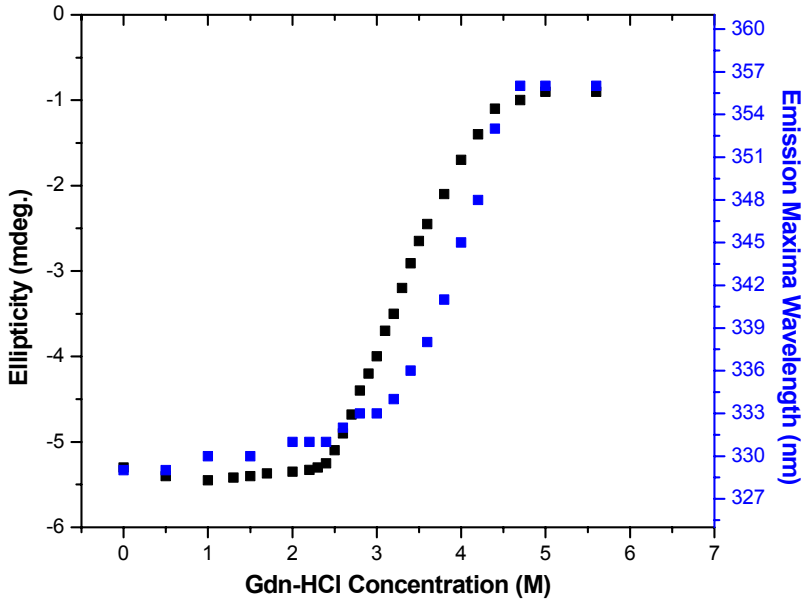

Figure 4.30: Plot of equilibrium unfolding data monitored by circular dichroism and fluorescence for 0.4 g/L RelBE. Black and blue squares represent CD and fluorescence data. Fluorescence excitation was at 295 nm in buffer 20 mM Tris, 150 mM NaCl, pH 8.

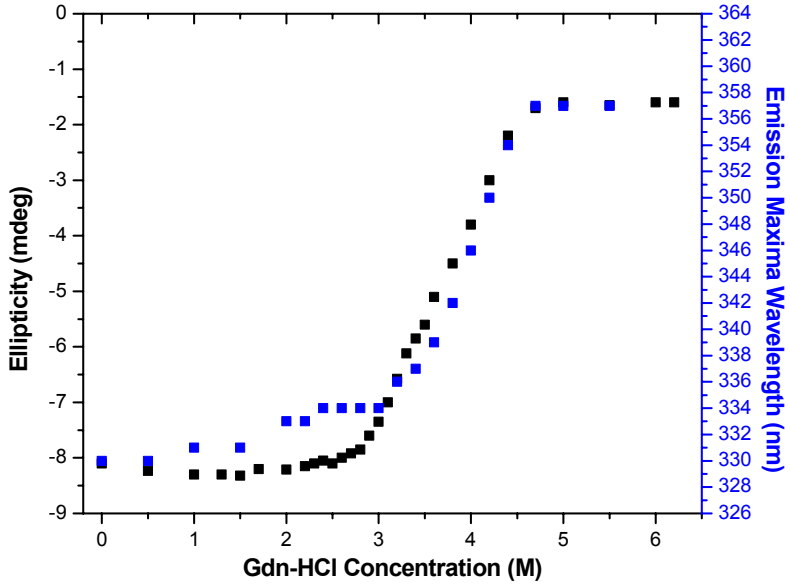

Figure 4.31: Plot of equilibrium unfolding data monitored by circular dichroism and fluorescence for 0.8 g/L RelBE. Black and blue squares represent CD and fluorescence data. Fluorescence excitation was at 295 nm in buffer 20 mM Tris, 150 mM NaCl, pH 8.

4.1.4. Temperature-induced unfolding

4.1.4.1. Circular dichroism

4.1.4.1.1. Antitoxin RelB unfolding

Thermal stability of RelB at 0.084 g/L was monitored by circular dichroism. Spectra were measured from 20 to 90 °C with steps of 10 °C (Figure 4.32).

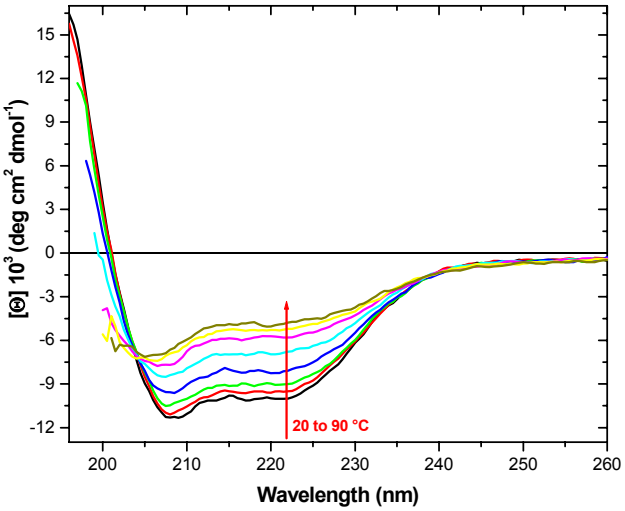

Figure 4.32: Thermal unfolding spectrums of RelB as measured by circular dichroism. CD spectra's were measured with 0.084 g/L RelB in PBS buffer, pH 7.4. Upward red arrow indicates the spectral shift with increase of temperature from 20 to 90 °C.

Wavelength of 220 nm was taken as selective marker to follow loss of secondary structure (Figure 4.32). At 0.084 g/L RelB in PBS buffer, pH 7.4, loss of negative ellipticity from ~-9.7· 10^3 to ~-4.5 · 10^3 deg·cm^2·dmol^{-1} was observed (Figure 4.33). Three sections can be seen in the melting curve, first between 20 and 50 °C, second from 50 to 70 °C, and the third from 70 to 90°C. Similarly, for 0.0084 g/L RelB curve was comparable except higher noise due to very low measured concentration (Figure 4.34). It is difficult to determine half transition temperatures from the CD melting curves.

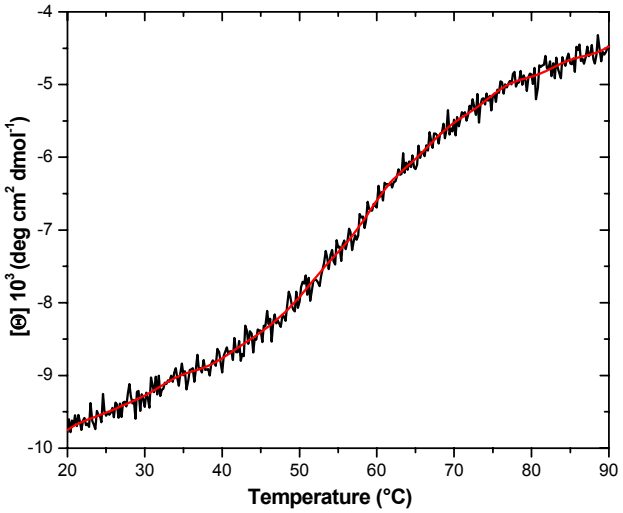

Figure 4.33: Thermal unfolding curve of 0.084 g/L RelB as monitored by change in ellipticity at selective wavelength of 220 nm by CD. CD ellipticity was measured at 220 nm in PBS buffer, pH 7.4. The molar ellipticity at 220 nm is plotted against increase in temperature.

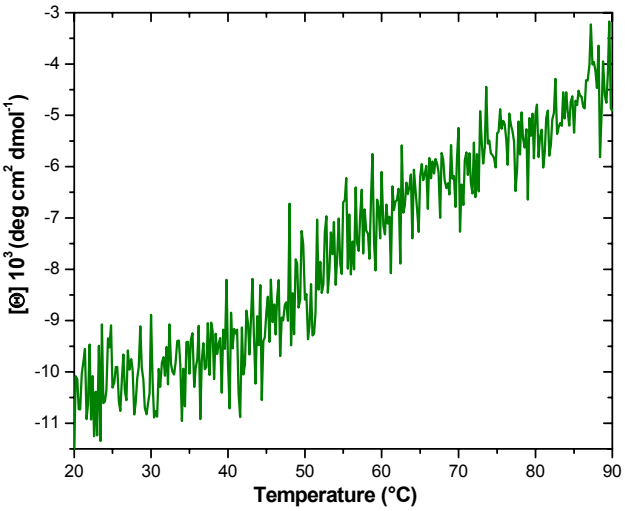

Figure 4.34: Thermal unfolding curve of 0.0084 g/L RelB as monitored by change in ellipticity at selective wavelength of 220 nm by CD. CD ellipticity was measured at 220 nm in PBS buffer, pH 7.4. The molar ellipticity at 220 nm is plotted against increase in temperature.

Reversibility of thermal melting was checked by slow cooling of the samples back to 20 °C from 90 °C. A near 100% reversibility of RelB was observed at 0.084 g/L concentration (Figure 4.35).

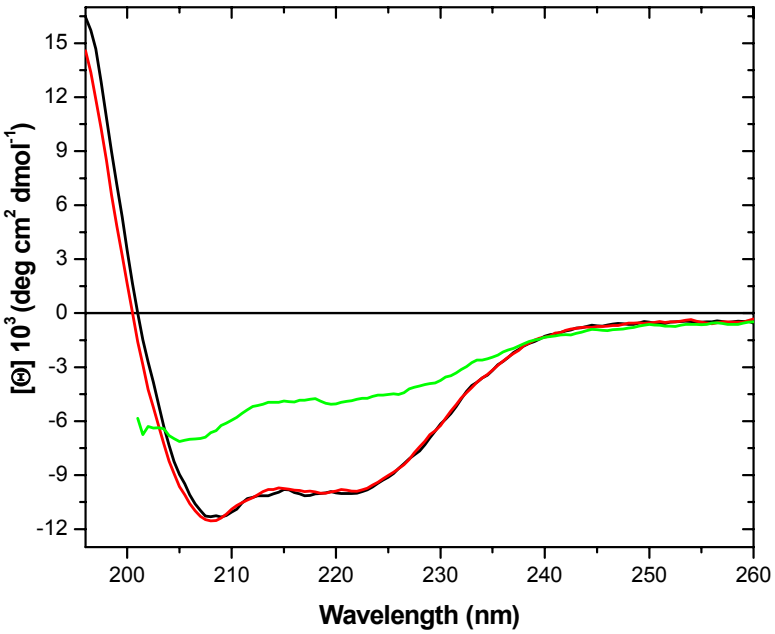

Figure 4.35: Selected thermal unfolding spectra of RelB (including renaturation spectrum). CD spectra were measured with 0.084 g/L RelB in PBS buffer, pH 7.4. Red, green and black lines indicate spectra's at 20, 90 and back to 20 °C (renaturation).

4.1.4.1.2. Toxin RelE and toxin -antitoxin RelBE complex unfolding

RelE thermal unfolding was quite similar to RelBE complex thermal unfolding in the way that no major changes in spectra was observed with increase in temperature (Figure 4.36 and 4.37). At higher temperatures precipitated protein can be seen in cuvette. After slow cooling to 20 °C, aggregates are visible. Both RelE and RelBE complex resulted in irreversible thermal denaturation.

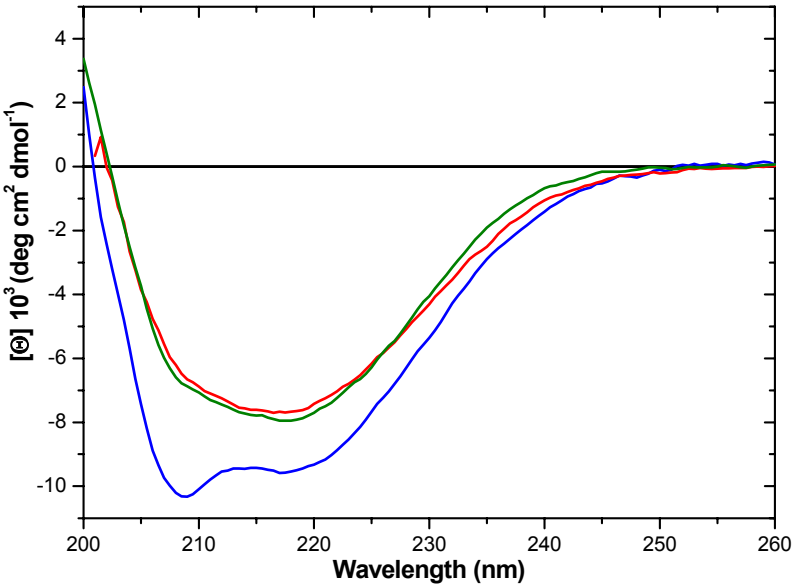

Figure 4.36: Selected thermal unfolding spectra of RelE (including back to 20 °C spectrum). CD spectra's were measured with 0.8 g/L RelE in PBS buffer, pH 7.4. Blue, green and red lines indicate spectra at 20, 90 and back to 20 °C.

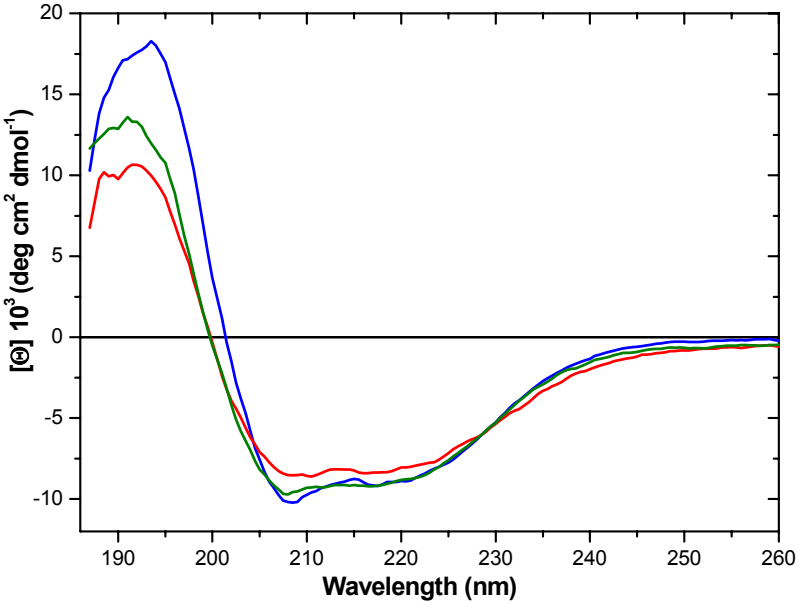

Figure 4.37: Selected thermal unfolding spectra of RelBE (including back to 20 °C spectrum). CD spectra were measured with 0.61 g/L RelBE in PBS buffer, pH 7.4. Blue, red and green lines indicate spectra at 20, 90 and back to 20 °C.

4.1.4.2 Differential scanning calorimetry (DSC)

The thermal unfolding of 0.3 g/L RelB has been examined by differential scanning calorimetry (Figure 4.38). A symmetrical curve was obtained and the classical two-state model was applied for the deconvolution of the experimental curve ($D_F \leftrightarrow D_U$). A transition temperature T_m of 60.72°C with an unfolding enthalpy ΔH^{cal} of 41.6 kcal/mol has been calculated from fitted curve. A second run after cooling of the sample from 90°C to 20°C indicated about ~81% reversibility of unfolding.

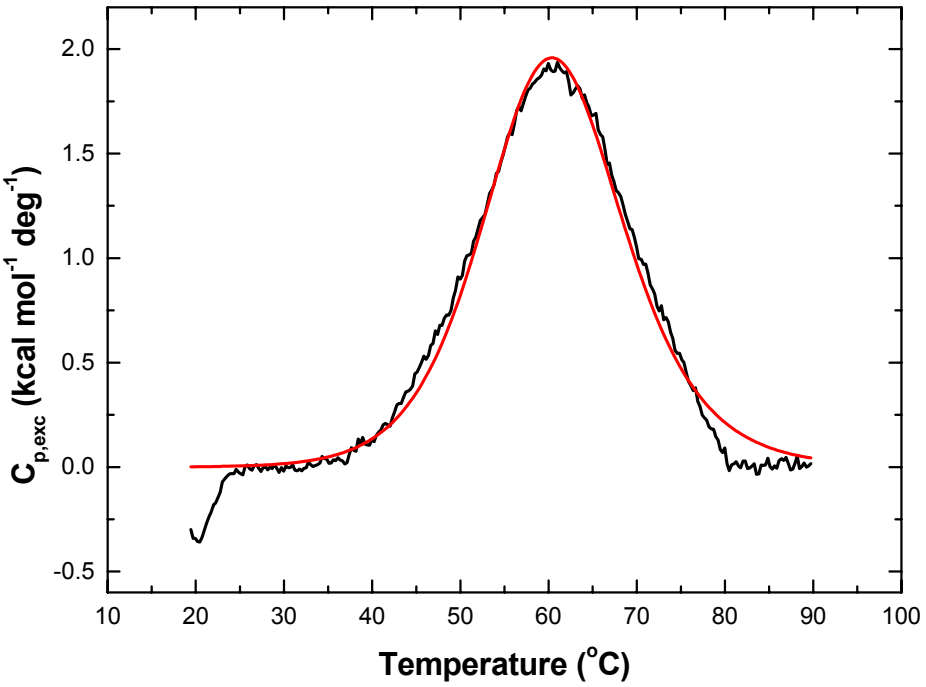

Figure 4.38: Raw and fit DSC curves of RelB. Best fit of the experimental DSC tracing obtained for (0.3 g/L) 16.7 µM $RelB_2$ in PBS buffer, pH 7.4. The corresponding red line is a fit performed according to a “two-state" model ($D_F \leftrightarrow D_U$).

4.2. Discussion

The RelBE addiction system in *E. coli* consists of two genes, *relB* and *relE*, encoding metabolically labile antitoxin RelB and stable toxin RelE, respectively. Ectopic expression of RelE in *E. coli* inhibits cell growth, reduces the number of colony-forming units and severely inhibits translation (*56, 57, 78*). Importantly, the *relBE* locus reduces the global level of translation during amino acid starvation (*57*). Therefore RelE is a global inhibitor of translation that is activated by nutritional stress. The degradation of labile RelB results in free stable RelE that exerts toxic effect to the cell. The regulation of the RelB cellular concentration is a major determinant of cell death. The production of the antitoxin must at least parallel that of the toxin to circumvent the induction of cell death. To achieve this, both proteins are encoded within a single operon, with the toxin gene always located directly downstream of the antitoxin gene. RelB forms a complex with RelE to inhibit its toxic effect and is also involved in the autoregulation of the *relBE* expression by binding to the *relBE* promoter. Therefore, RelB was considered to be consisted of at least two functional domains: the DNA-binding domain and the RelE binding domain. But the recent data from the crystal structure analysis of archaeaon *Pyrococcus horikoshii* RelBE revealed a unique structure where the toxin RelE contains a single globular domain with an unusual fold, whereas the antitoxin RelB has no hydrophobic core and wraps around the toxin. This suggests that the antitoxin has a defined structure only when bound to the toxin. In addition, the lack of tertiary structure could make the unbound RelB easy prey for the ATP-dependent Lon protease, thus explaining the short half-life of the antitoxin. Similarly, the antitoxin MazE from equivalent system MazEF also has a long unstructured extension that wraps around a dimer of the MazF toxin.

RelE cleaves mRNA positioned at the ribosomal A-site *in vitro* (*105*) and *in vivo* (*104*). Six histidines tagged RelE is able to interact with RelB and bind to the

relBE promoter and has the same activity as native RelE (*78, 105*). Therefore six histidines tags appear to have no effects on the function of RelB and RelE *in vitro*. In all our experiments, we used six histidines tagged RelE. Efficient inhibition of the toxic activity of RelE by the RelB antitoxin is essential for maintaining the viability of bacteria but while starting the work mentioned in this report little concrete information concerning the molecular mechanism of this inhibition was available. This is partially true till date aswell.

Is antitoxin RelB a natively unfolded protein???

To our surprise, recombinant purified RelB revealed a high amount of secondary structural elements. The secondary structural content as calculated from our CD spectra shows a modest 41% α-helical content (Figure 4.1 and Table 4.1). Our data reconciles with the theoretical belief following RelB having at least two functional domains, one for DNA binding and other for RelE binding. However, this observation significantly differs with the published crystal structure of *Pyrococcus horikoshii* RelB in RelBE complex where RelB is found to be lacking a hydrophobic core and extensively wrapped around RelE (*108*); by proposal in the paper; in the absence of RelE partner RelB should be an unfolded or more precisely natively unfolded protein. Our results contradict this proposal as they clearly show a well structured protein that exists in a concentration dependent monomer-dimer equilibrium and surprisingly enough refolds almost quantatively upon thermal unfolding. One hypothesis can be followed as RelB is supposedly an unstable partner of RelE, and having a structure lacking hydrophobic core in the complex makes it a destabilized protein as alone (easy prey to Lon protease) which in turn a well folded structure when expressed from a clone expressing only RelB and having virtuous secondary structural contents in solution. Only explanation to our mind could be having variable flexibility in RelB protein either in the absence or in the vicinity of RelE molecule. It is not known whether the formation of RelBE complex blocks the

RelB Lon protease degradation by sterically occluding interactions of RelB or if the formation of the RelBE complex alters the structure of RelB in a way that prevents the action of Lon protease on RelB. Latter argument is intriguing and supports our explanation. Were this alteration of structure to involve a major portion of RelB, then this could serve as the mechanism of toxin neutralization as well.

On the other hand, RelE found to be having higher amount of β-sheets than helices. Secondary structure contents of RelBE complex shows a modest average of observed RelB and RelE secondary structure elements.

The size exclusion chromatography and analytical ultracentrifugation results presented in this report revealed that RelB and RelE in the lowest measured concentration range interact directly to form a heterodimeric complex in solution. The complex stoichometry seems to be a highly concentration dependent phenomenon. In our size exclusion chromatography experiments RelBE heterodimeric and heterotetrameric complexes were observed (Figure 4.6). Analytical ultracentrifugation experiments also revealed equilibrium between RelBE heterodimeric and heterotetrameric complexes pointing to a dissociation constant roughly in μM range (Figure 4.9). Our results in solution are in agreement with the stoichometry observed in crystal structure of *Pyrococcus horikoshii* RelBE complex at higher concentration (*108*). RelB and RelE proteins in solution are found to be dimeric at higher concentration ranges as measured by both techniques, only at low concentration of ~0.07 g/L equilibrium molar masses between dimer and monomer have been observed by size exclusion chromatography (Figure 4.4 and 4.5). Overall, these observations points towards 1:1 ratio of RelB and RelE proteins to form a stable complex in solution. Dimerization of toxin and antitoxin were found to be a common denominator of TA systems like MazEF from *E. coli* or RelBE from *Pyrococcus horikoshii*. RelB dimerization is also supported by the evidence that *in vivo* it binds to promoter

DNA (*79*), and incidently many of the DNA binding proteins are dimer (*79, 196-199*).

Energetics of the RelBE structure

The stability curves of RelB, RelE and RelBE complex were measured by using Gdn-HCl or heat as a denaturing agent. Gdn-HCl denaturation unfolding measurements were followed by changes monitored in both the far ultraviolet circular dichroism and intrinsic fluorescence emission. Circular dichroism technique predominantly measures changes in the secondary structure of proteins whereas intrinsic fluorescence emission predominantly hints towards changes in tertiary structure. In equilibrium experiments measured by either technique, RelB, RelE and RelBE complex denatured cooperatively in a mechanism that differs significantly with the commonly known globular proteins two-state unfolding mechanisms.

The denaturation unfolding stability curves obtained for RelB and RelE irrespective of method applied to monitor, either CD or fluorescence (only RelE) point towards a concentration dependent unfolding process. Denaturant unfolding of RelB was followed by circular dichroism only, as RelB contains no tryptophan. RelB and RelE are dimers at higher concentrations similar to MazE of MazEF and εξ TA systems where components are also dimers and show two state unfolding mechanisms (*103, 200*). Concentration dependence is evident from the Gdn-HCl denaturation curves measured at different concentrations. However, at low concentration curves direct towards presence of intermediates. With increase in protein concentration denaturant stability of dimer protein increases and leads to coupled dissociation-unfolding process. The experimental curves were fitted with the model assuming “Two-state monomer” and “Two state dimer” unfolding mechanism (Figure 4.10 to 4.15). Thermodynamic parameters, ΔG, C½, and *m* were calculated from the applied models for RelB and RelE.

Unfolding studies monitoring circular dichroism showed that the antitoxin RelB has a significantly lower stability than the toxin RelE. A shift in protein stability against denaturant has been observed which amounts to ~1 M Gdn-HCl in both RelB and RelE; low and high concentrations. A significant difference in model calculated ΔG values were observed, as apparent monomer unfolding results in significantly lower ΔG values than dimer unfolding (Table 4.2). ΔG values obtained for dimer denaturation of RelB and RelE are in reasonable agreement with the calculated ΔG values of other dimeric proteins (*197*). For instance, calculated ΔG value for RelB unfolding amounts to ~10 kcal/mol which is in good agreement with other similar small size protein like Arc repressor from bacteriophage p22 (*194*).

Tryptophan containing RelE fluorescence emission spectra showed a red shift with increasing Gdn-HCl concentration, which has been the common observation in protein denaturation by denaturant. The usual interpretation of the red shift of the fluorescence of the single tryptophan residue in this case was that denaturation progressively exposed tryptophan to the solvent. In its native conformation, at 0 M Gdn-HCl in buffer, the maximum emission wavelength of dimeric RelE was 328 nm however with decrease in protein concentration which corresponds to near monomer concentration a marginal blue shift to 325 nm was observed (Figure 4.22 and 4.23). These wavelengths suggest that the tryptophan residue of the RelE is in strict hydrophobic environment. Harvesting this property of RelE we were able to study its denaturant stability. Irrespective of concentrations measured, the red shift of wavelength emission was consistent, only shift in denaturant stability has been observed.

In summary, we propose the following models for the unfolding process of RelB and RelE induced by Gdn-HCl and monitored by circular dichroism and fluorescence spectroscopy in our experimental conditions:

$N \leftrightarrow D$;
Monomer unfolding mechanism applicable to both RelB and RelE measured at lower protein concentrations.

$N_2 \leftrightarrow 2D$;
Dimer unfolding mechanism applicable to both RelB and RelE measured at higher protein concentrations.

where N is native monomer and N_2 is native dimer; and D corresponds to denatured state.

The ΔG calculated for RelE from the denaturant unfolding measurements monitored by either CD or fluorescence is in reasonable agreement with each other (Table 4.2.). The calculated thermodynamic parameters are the apparent approximate values, obtained by model analysis based on the results obtained from size exclusion chromatography and analytical ultracentrifugation experiments. As near monomer and near dimer states have been observed, which could be consisted of major amount monomers and dimers in their respective concentrations but presence of higher or lower oligomeric forms cannot be ruled out from the obtained results. Therefore calculated thermodynamic parameters should be considered as approximate values only. A strong conclusion of the presented study is that at high protein concentration the dissociation/unfolding are a highly cooperative process and stabilization by dimerization increases the structural stability of RelB and RelE significantly.

Denaturant unfolding of RelBE complex measured by CD or intrinsic fluorescence emission reveals a marginal concentration dependence as observed between measured concentration ranges, which results in varying $C_{½}$ values and steepness of the curves. The dissimilarity in denaturation curves monitored by CD or fluorescence indicates that changes in environment of the

single tryptophan of RelE in RelBE complex and changes in RelBE secondary structure do not occur concurrently and this result points to the formation of intermediates (Figure 4.29 to 4.31). In all measured concentrations, slope of RelBE measured by fluorescence emission is similar but half transition concentration is higher than those obtained from circular dichroism. Because, tryptophan might be buried deep inside the RelBE complex, and slight changes in secondary structure conformation prior to RelBE complex unfolding are necessary before tryptophan started getting exposed. Denaturant molar concentrations are nearly same when plateau values of transition curve were achieved. So this evidences direct towards stability of RelBE complex in which RelE seems to be a major component contributing to increased stability of complex. The loss of secondary structure bit earlier than changes in fluorescence emission can be interpreted as the lower stability of RelB component in the complex. The explanation is supported by the denaturant unfolding of individual components *i.e.* RelB and RelE at different protein concentrations where RelB shows a low denaturant stability compared to RelE. The calculation of thermodynamic parameters of RelBE complex by denaturant unfolding model analysis was not possible. The system contains two different proteins having different denaturant stability as individuals. At the studied concentrations of RElBE complex the unfolding curves do not show dissociation of the complex or unfolding of components as individual processes. Rather dissociation and unfolding seemed to be coupled process that cannot be distinguished by the available data. Adding to complexity the RelBE complex showing concentration dependence in terms of heterodimeric or heterotetramic complex at different concentration and measured unfolding curves pointing to very complex mechanisms. Therefore, precise calculation of thermodynamic parameters was not possible for us. Only a qualitative evaluation of the RelBE complex unfolding data can be and has been described here. No reliable conclusion can be made for the thermal melting of RelE and RelBE complex analysed by circular dichroism and differential scanning calorimetry (Figure 4.36 and 4.37). Both

techniques did not provide reliable results as RelE and RelBE strongly aggregated or precipitated around 50 °C during thermal unfolding under all tested experimental conditions. The aggregation which was quite evident by looking at data obtained and even it was possible to see precipated protein by eye after cooling.

Surprisingly thermal induced unfolding of RelB seems to be a highly reversible process (Figure 4.32). Thermal melting was measured by circular dichroism and differential scanning calorimetry. CD signal intensity measured at 220 nm results in too broad transitions and unavailability of plateau value makes it nearly impossible to determine the precise transition temperature values and so other thermodynamic parameters. Only a qualitative assessment could be done which shows a substantial loss of secondary structure with the increase in temperature and most importantly nearly 100% gain of secondary structure contents after cooling back to start temperature. Whereas excessive heat capacity curves for RelB measured by differential scanning calorimetry provided a good fit with assumption of two-state mechanism where native dimers unfolds into unfolded dimers ($D_F \leftrightarrow D_U$) resulted in a transition temperature, T_m of 60.7 °C with an unfolding enthalpy, ΔH^{cal} of 41.6 kcal/mol (Figure 4.38). The measurements were done in apparent dimeric concentrations, the excessive heat capacity curves are characterized by symmetric peaks, suggesting that dissociation phenomena do not contribute remarkably to the melting process at the concentration of the DSC experiments. The proteins were near dimers at the low temperature of the starting conditions and did not seem to dissociate at high temperatures. An asymmetric melting curve would be expected if native RelB dimers melted in unfolded monomers. But the possibility of mixtures of RelB dimers and monomers cannot be ignored at start temperatures or otherway possibilities of intermediates cannot be excluded while melting. Therefore precise model of unfolding cannot be deduced due to weak oligomeric state data. Regardless of weak data, a strong conclusion can be drawn that RelB is a folded

protein and denatures from folded to unfolded state very similarly to other dimeric proteins, despite of various beliefs that it is supposedly natively unfolded protein (*108*).